Gravitational lensing by naked singularities

K. S. Virbhadra*

*Department of Applied Mathematics, University of Cape Town, Rondebosch 7701, South Africa
and Physics and Mathematics Departments, Duke University, Durham, North Carolina 27708*

G. F. R. Ellis†

Department of Applied Mathematics, University of Cape Town, Rondebosch 7701, South Africa

We model massive dark objects in galactic nuclei as spherically symmetric static naked singularities in the Einstein massless scalar field theory and study the resulting gravitational lensing in detail. Based on whether or not a naked singularity is covered within a photon sphere we classify naked singularities into two kinds: *weakly naked* (those contained within at least one photon sphere) and *strongly naked* (those not contained within any photon sphere). The qualitative features of gravitational lensing due to a weakly naked singularity are similar to those due to a Schwarzschild black hole (these give rise to one Einstein ring but no radial critical curve). However, the gravitational lensing due to a strongly naked singularity is qualitatively different from that due to a Schwarzschild black hole; a strongly naked singularity gives rise to either two or nil Einstein ring(s) and one radial critical curve. A light ray passing close to a photon sphere of a black hole or a weakly naked singularity goes around its photon sphere once, twice, or many times (before reaching an observer) depending upon the impact parameter and thus gives rise to a sequence of theoretically infinite number of relativistic images, which are highly demagnified. A strongly naked singularity produces no relativistic images.

I. INTRODUCTION

This paper considers how gravitational lensing studies might possibly distinguish between Schwarzschild black holes, and the naked singularities that can occur for example if there is a massless scalar field present in a spherically symmetric spacetime. We find that the key issue determining the nature of lensing is whether or not there is a photon sphere surrounding the singularity.

There has been extensive research work on black holes and naked singularities, and in particular on whether the cosmic censorship hypothesis is valid (for references see [1–5]), but not much attention has been paid to how naked singularities could be observationally distinguished from black holes. Given that no proof is known for the cosmic censorship hypothesis, and the importance of this hypothesis for gravitational physics [4], it is a worthwhile research project to investigate the distinctive observational features of naked singularities and black holes. This is particularly so because it has been stated by Penrose that " . . . it might be the case that cosmic censorship requires a zero (or at least a nonpositive) cosmological constant" [4], and the studies of *type Ia* supernovae indicate a positive cosmological constant [6]. As this data have alternatively been taken as evidence for a time-varying dark energy, sometimes called "quintessence" [7], which currently dominates the expansion of the universe, it is worth carrying out these investigations in a context where classical scalar fields can play a significant role.

Virbhadra *et al.* [8] initiated a research project that uses gravitational lensing as a tool to address this problem theoretically. They carried out some preliminary studies of this subject. In this paper we extend that work and study distinctive lensing features of black holes and naked singularities in detail. We obtain a photon sphere equation for a general static spherically symmetric metric. We term a naked singularity *weakly naked* if it is covered by at least one photon sphere; else we call it *strongly naked*. We model massive dark objects at galactic centers first as Schwarzschild black holes, and secondly as weakly as well as strongly naked singularities described by the Janis, Newman and Winicour (JNW) spherically symmetric spacetime. We study gravitational lensing in detail in each case. We find that the Schwarzschild black holes and weakly naked singularities share the same qualitative lensing features, whereas they differ substantially from the lensing characteristics of strongly naked singularities. Throughout this paper we use geometrized units.

II. LENS EQUATION, MAGNIFICATION, CRITICAL CURVES AND CAUSTICS

A lens equation which allows for large bending of light near a lens may be expressed as [9]

$$\tan\beta = \tan\theta - \alpha, \tag{1}$$

with

$$\alpha \equiv \frac{D_{ds}}{D_s}[\tan\theta + \tan(\hat{\alpha} - \theta)], \tag{2}$$

where β and θ, respectively, stand for angular positions of an unlensed source and an image measured from the optic axis (the reference line joining the center of the lens and the ob-

*Email address: shwetket@phy.duke.edu
†Email address: ellis@maths.uct.ac.za

server). $\hat{\alpha}$ is the Einstein bending angle. D_{ds} and D_s are the angular diameter distances of the deflector (lens) and the source, respectively, from the observer. The source and observer are assumed to be situated at a large distance from the lens so that the gravitational field due to the lens on them is negligible. The impact parameter, i.e., the perpendicular distance from the center of the lens to the tangent to the null geodesic at the source, is (see Fig. 1 in [9])

$$J = D_d \sin \theta. \tag{3}$$

The deflection of light in a gravitational field causes a change in the cross section of a bundle of rays; however, the surface brightness is preserved according to Liouville's theorem. Therefore, the magnification of an image (i.e., the ratio of the flux of the image to the flux of the unlensed source) turns out to be the ratio of the solid angles of the image and of the unlensed source made at the observer. Thus the magnification μ of an image formed due to a circularly symmetric gravitational lensing is

$$\mu = \left(\frac{\sin \beta}{\sin \theta} \frac{d\beta}{d\theta} \right)^{-1}. \tag{4}$$

The radial and tangential magnifications are given by

$$\mu_r \equiv \left(\frac{d\beta}{d\theta} \right)^{-1}, \quad \mu_t \equiv \left(\frac{\sin \beta}{\sin \theta} \right)^{-1} \tag{5}$$

and singularities in these quantities in the image plane give *radial critical curves* (RCCs) and *tangential critical curves* (TCCs), respectively. The corresponding values in the source plane are known as *radial caustics* (RCs) and the *tangential caustic* (TC), respectively. It is clear that $\beta = 0$ gives the TC and the corresponding values of θ are the TCCs. The sign of the magnification μ of an image gives the parity of the image and critical images are defined as images of 0 parity. Frittelli, Kling, and Newman [10] studied gravitational lensing in Schwarzschild spacetime using a different approach and they noted that the lens equation (1) proposed by us in [9] works remarkably well.

The lens equation (1) and the expression for magnification (4), for small values of angles β, θ and $\hat{\alpha}$, become respectively

$$\beta = \theta - \frac{D_{ds}}{D_s} \hat{\alpha} \tag{6}$$

and

$$\mu = \left(\frac{\beta}{\theta} \frac{d\beta}{d\theta} \right)^{-1} \tag{7}$$

which have been much used in the literature to study gravitational lensing due to light deflection in a weak gravitational field (see [11] and references therein).

III. LIGHT DEFLECTION ANGLE, PHOTON SPHERE EQUATION, AND CLASSIFICATION OF NAKED SINGULARITIES

A general static spherically symmetric spacetime may be expressed by the line element

$$ds^2 = B(r)dt^2 - A(r)dr^2 - D(r)r^2(d\vartheta^2 + \sin^2\vartheta d\varphi^2). \tag{8}$$

The bending angle of a light ray in a general static spherically symmetric spacetime, described by the line element (8), for a closest distance of approach r_0 is given by [8]

$$\hat{\alpha}(r_0) = 2 \int_{r_0}^{\infty} \left(\frac{A(r)}{D(r)} \right)^{1/2} \left[\left(\frac{r}{r_0} \right)^2 \frac{D(r)}{D(r_0)} \frac{B(r_0)}{B(r)} - 1 \right]^{-1/2} \frac{dr}{r} - \pi \tag{9}$$

and the impact parameter J is

$$J = r_o \sqrt{\frac{D(r_o)}{B(r_o)}}. \tag{10}$$

A photon sphere in a static spherically symmetric spacetime is defined as a timelike hypersurface $\{r = r_{ps}\}$ if the Einstein bending angle of a light ray with the closest distance of approach r_0 becomes unboundedly large as r_0 tends to r_{ps} [9]. Thus a photon sphere equation for a general static spherically symmetric metric follows from Eq. (9):

$$2D(r)B(r) + r\frac{dD(r)}{dr}B(r) - r\frac{dB(r)}{dr}D(r) = 0. \tag{11}$$

Out of many possible solutions of the above equation for a given metric one considers only $\{r = \text{const}\}$ timelike hypersurfaces as photon spheres. For the Schwarzschild metric the above equation readily gives the photon sphere at $\{r = 3m\}$. An alternative definition of a photon sphere is given in [12], which yields the same photon sphere equation (11) given above.

A naked singularity may or may not be covered within a photon sphere. The existence or nonexistence of a photon sphere with a spacetime acting as a gravitational lens has important implications for gravitational lensing. Therefore we classify naked singularities in two categories:

Weakly naked singularities (WNS). Naked singularities contained within at least one photon sphere are termed weakly naked singularities.

Strongly naked singularities (SNS). Naked singularities which are not covered within any photon spheres are termed strongly naked singularities.

In the next section we will show some interesting different characteristics of the SNS against the WNS and Schwarzschild black holes.

IV. DISTINCTIVE FEATURES OF WEAKLY AND STRONGLY NAKED SINGULARITIES

Janis, Newman and Winicour obtained the most general static spherically symmetric solution to the Einstein massless scalar equations ($R_{ij} = 8\pi\Phi_{,i}\Phi_{,j}$ with $\Phi_{,i}^{;i} = 0$, where R_{ij} is

the Ricci tensor and Φ is the massless scalar field). This solution [14,15,20] is given by the line element

$$ds^2 = \left(1 - \frac{b}{r}\right)^{\nu} dt^2 - \left(1 - \frac{b}{r}\right)^{-\nu} dr^2 - \left(1 - \frac{b}{r}\right)^{1-\nu}$$

$$\times r^2 (d\vartheta^2 + \sin^2\vartheta \, d\varphi^2) \tag{12}$$

and the scalar field

$$\Phi = \frac{q}{b\sqrt{4\pi}} \ln\left(1 - \frac{b}{r}\right), \tag{13}$$

where

$$\nu = \frac{2M}{b}, \quad b = 2\sqrt{M^2 + q^2}. \tag{14}$$

M and q, the Arnowitt-Deser-Misner (ADM) mass and the scalar charge are constant real parameters in this solution. For $q=0$ this solution reduces to the Schwarzschild solution. The Einstein tensor for the JNW metric is

$$G^a_b = 8\pi \begin{pmatrix} \rho(r) & 0 & 0 & 0 \\ 0 & -p_1(r) & 0 & 0 \\ 0 & 0 & -p_2(r) & 0 \\ 0 & 0 & 0 & -p_2(r) \end{pmatrix} \tag{15}$$

for

$$\rho(r) = p_1(r) = -p_2(r) = \frac{b^2(1-\nu^2)\left(1 - \frac{b}{r}\right)^{\nu}}{32\pi r^2(r-b)^2}. \tag{16}$$

Thus the JNW metric has positive energy density ρ and radial pressure p_1, and negative transverse pressures p_2 for all values of $r : b < r < \infty$. The JNW spacetime satisfies the weak energy condition and it has a globally naked strong curvature singularity (in the sense of Tipler et al.) at $r=b$ for $q \neq 0$ (see [16] with [13]).

For the JNW metric Eq. (9) gives the light deflection angle

$$\hat{\alpha}(r_0) = 2 \int_{r_0}^{\infty} \frac{dr}{r\sqrt{1 - \frac{b}{r}}\sqrt{\left(\frac{r}{r_0}\right)^2 \left(1 - \frac{b}{r}\right)^{1-2\nu}\left(1 - \frac{b}{r_0}\right)^{2\nu-1} - 1}} - \pi \tag{17}$$

and Eq. (10) gives the impact parameter

$$J(r_0) = r_o \left(1 - \frac{b}{r_0}\right)^{(1-2\nu)/2}. \tag{18}$$

According to Eq. (11), the only photon sphere for the JNW metric is at the radial distance

$$r_{ps} = \frac{b(1+2\nu)}{2}. \tag{19}$$

The metric (12) has a photon sphere only for $1/2 < \nu \leq 1$, i.e., for $0 \leq (q/M)^2 < 3$ (see also in [12]). We define the impact parameter of a photon sphere, denoted by J_{ps}, as the value for J as r_0 tends to r_{ps}. Thus one has

$$J_{ps} = M\left(\frac{1+2\nu}{\nu}\right)\left(1 - \frac{2}{1+2\nu}\right)^{(1-2\nu)/2}. \tag{20}$$

In Fig. 1 (left) we plot the coordinate radii of the photon sphere [the right-hand side of Eq. (19)] and the curvature singularity $(r=b)$ vs the square of the scalar charge (all
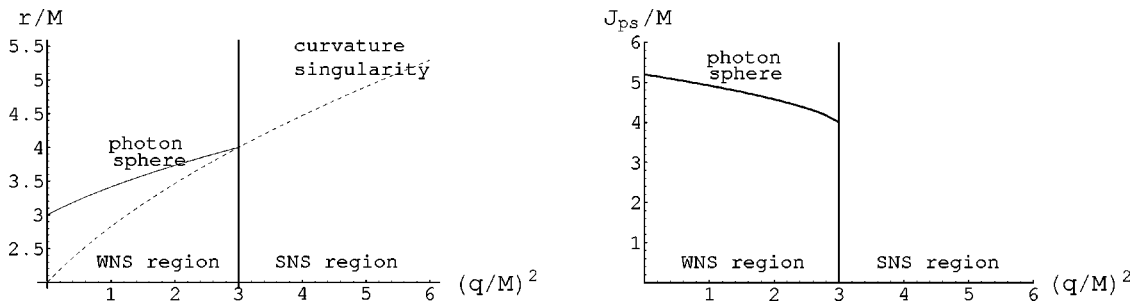

FIG. 1. The coordinate radii of the photon sphere and the curvature singularity of the JNW spacetime $[(q/M)^2 > 0]$ are plotted against the square of the scalar charge (left). The impact parameter of the photon sphere is plotted against the square of the scalar charge (right). All these quantities are expressed in terms of the ADM mass M. The vertical lines at $(q/M)^2 = 3$ in both figures separate the weakly naked singularities region $[0 < (q/M)^2 < 3]$ from the strongly naked singularities region $(q/M)^2 \geq 3$.

FIG. 2. The relative sizes of photon spheres expressed by J_{ps}/M are depicted, starting from the left-hand side, for $(q/M)^2=0$ (Schwarzschild black hole), 1 (WNS), and 2.99 (WNS). The black dots denote curvature singularities. As $(q/M)^2$ increases the size of a photon sphere decreases. For $(q/M)^2 \geq 3$ (SNS) there are no photon spheres, which is expressed in the figure by a bare black dot on the extreme right-hand side.

these quantities scaled in terms of the ADM mass M); both increase with an increase in $(q/M)^2$ and meet at $(q/M)^2=3$. For $0<(q/M)^2<3$ there is always one photon sphere which covers the naked singularity and therefore these singularities are weakly naked; however for $(q/M)^2 \geq 3$ the singularities are not covered by any photon sphere and therefore these are strongly naked. In Fig. 1 (right) we plot the impact parameter of the photon sphere against the square of the scalar charge. J_{ps} is real only for $0 \leq (q/M)^2<3$ and it decreases monotonically in this range with an increase in the value of $(q/M)^2$. One has $\lim_{(q/M)^2 \to 3} J_{ps}=4M$.

In Fig. 2 we show the relative sizes (expressed by J_{ps}/M) of photon spheres for the Schwarzschild black hole and WNS. As the value of $(q/M)^2$ increases the size of the photon sphere decreases. For SNS $[(q/M)^2 \geq 3]$ there are no photon spheres and therefore these singularities are not covered by any such spheres.

Some properties of WNS and SNS can also be seen through the geodesic equations. The geodesics in the gravitational field of a Schwarzschild black hole and any weakly naked JNW singularity have similar qualitative features, whereas those due to any strongly naked JNW singularity differ from them. This is shown below.

Null geodesics in the JNW spacetime are governed by the equation

$$\frac{d^2r}{dk^2}=\left(r-\frac{b(1+2\nu)}{2}\right)\left\{\left(\frac{d\vartheta}{dk}\right)^2+\sin^2\vartheta\left(\frac{d\varphi}{dk}\right)^2\right\} \quad (21)$$

where k is an affine parameter along the geodesic.

First consider the case of WNS ($1/2<\nu<1$). These have one photon sphere at $r=b(1+2\nu)/2$. The right side of Eq. (21) is negative, zero and positive respectively for r less than, equal to and greater than $b(1+2\nu)/2$. It is obvious from Eq. (21) that any future endless null geodesic starting at any point with $r:b<r<b(1+2\nu)/2$ and initially directed inwards (i.e., dr/dk is initially negative) will continue inwards and will end at the naked singularity $r=b$. However any future endless null geodesic at any point outside the photon sphere [i.e., $b(1+2\nu)/2<r<\infty$] and initially directed outwards (i.e., dr/dk is initially positive) will continue outwards and escape to infinity. It is also obvious from Eq. (21) that any null geodesic initially tangent to the photon sphere will continue in the sphere. It is known that all these facts are also true for the case of the Schwarzschild black hole (see [12] and references therein).

For SNS ($0 \leq \nu \leq 1/2$), $r>b(1+2\nu)/2$ for all values of r in the JNW spacetime and therefore the right side of Eq. (21) is always positive. Thus it is evident that any future endless null geodesic at any point in the JNW spacetime initially directed outwards or inwards (i.e., dr/dk is initially positive or negative) will finally escape to infinity.

Timelike geodesics in the JNW spacetime are given by the equation

$$\frac{d^2r}{ds^2}=\left(r-\frac{b(1+2\nu)}{2}\right)\left\{\left(\frac{d\vartheta}{ds}\right)^2+\sin^2\vartheta\left(\frac{d\varphi}{ds}\right)^2\right\}$$
$$-\frac{M}{r^2}\left(1-\frac{b}{r}\right)^{\nu-1} \quad (22)$$

where s stands for the arc length along the geodesic.

For the Schwarzschild black hole as well as WNS geometries one may get circular timelike geodesics ($d^2r/ds^2=0$) outside the photon sphere. For $b<r \leq b(1+2\nu)/2$, $d^2r/ds^2<0$ and therefore any future timelike geodesic starting at some point in this range of radial coordinate and initially directed inward (i.e., $dr/ds<0$) will continue inwards.

For the SNS geometries $r>b(1+2\nu)/2$ and therefore the first term on the right side of Eq. (22) is always positive for nonradial geodesics whereas the second term is always negative; therefore one may organize these two terms to cancel to give timelike circular geodesics in SNS spacetimes.

Now we discuss the behavior of the bending angle $\hat{\alpha}$ for the Schwarzschild black hole, WNS, and SNS. One has $\lim_{r_0 \to \infty} \hat{\alpha}(r_0)=0$ for all values of ν, $\lim_{r_0 \to r_{ps}} \hat{\alpha}(r_0)=\infty$ for $1/2<\nu \leq 1$ (Schwarzschild black hole and weakly naked singularities) and $\lim_{r_0 \to b} \hat{\alpha}(r_0)=-\pi$ for $0 \leq \nu \leq 1/2$ (strongly naked singularities).

In Fig. 3 we plot the bending angle $\hat{\alpha}$ against the impact parameter J (scaled in terms of the ADM mass M) for several values of ν. In the top left figure we plot curves for $\nu=1$ (Schwarzschild black hole) and $\nu=0.8,0.6$ (WNS). It is obvious that these share similar qualitative features; the bending angle strictly increases with a decrease in the impact parameter and becomes unboundedly large as the impact parameter approaches the impact parameter for their respective photon spheres (i.e., $J \to J_{ps}$). Thus lensing by WNS would not give rise to a radial critical curve, instead they would give relativistic Einstein rings [21] (when the source, lens and observer are aligned) as in the case of the Schwarzschild
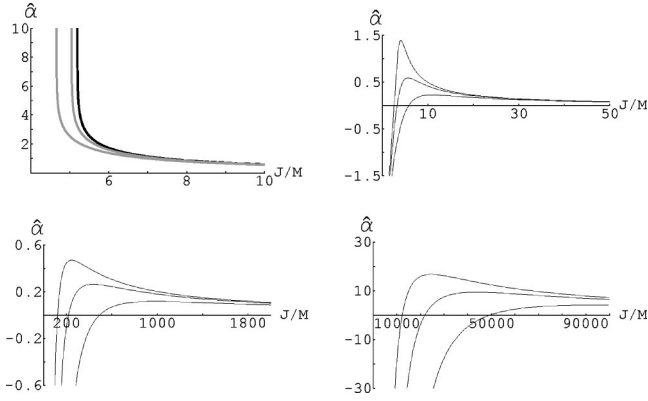
FIG. 3. The light deflection angle $\hat{\alpha}$ is plotted against the impact parameter J (expressed in terms of the ADM mass M) for ν $=1,0.8,0.6$ (top left), $\nu=0.4,0.3,0.2$ (top right), $\nu=0.04,0.03,0.02$ (bottom left), and $\nu=0.004,0.003,0.002$ (bottom right). In the top left figure the dark curve is for $\nu=1$ (Schwarzschild black hole) whereas the faint curves are for $\nu=0.8,0.6$ (weakly naked singularities) in the decreasing order of ν from the right. All other plots (top right, bottom left and bottom right) are for strongly naked singularities (the larger the value of ν the larger is the maximum deflection angle); for these cases the deflection angle $\hat{\alpha}$ approaches $-\pi$ as the impact parameter J tends to be zero. The deflection angle $\hat{\alpha}$ is expressed in radian (top left and right), degree (bottom left), and arcsecond (bottom right).

TABLE I. Maximum deflection angle and impact parameter. The symbols ° and ″ stand for the degree and arcsecond respectively.

ν	$\dfrac{q}{M}$	$\hat{\alpha}_{max}$	$\dfrac{J}{M}$
0.45	1.98451	132.50°	3.789810
0.40	2.29129	79.690°	4.032070
0.35	2.67643	51.591°	4.608901
0.30	3.17980	33.711°	5.645745
0.25	3.87298	21.486°	7.479242
0.20	4.89898	12.908°	10.95126
0.15	6.59124	6.9364°	18.54303
0.10	9.94987	2.9887°	40.33053
0.05	19.9750	0.7338°	158.1231
0.04	24.9800	0.4687°	246.4559
0.03	33.3180	0.2632°	437.3710
0.02	49.9900	0.1168°	982.8168
0.01	99.9950	0.0292°	3928.199
0.005	199.997	26.264″	15709.03
0.004	249.998	16.809″	24543.71
0.003	333.332	9.4547″	43631.29
0.002	499.999	4.2020″	98175.33
0.001	999.999	1.0505″	392704.1

impact parameter increases.

black hole lensing [9]. In Fig. 3 (top right) we plot for ν $=0.4$ (the uppermost), $\nu=0.3$ (the middle), and $\nu=0.4$ (the lowermost) and these are for SNS. $\hat{\alpha}$ first increases with a decrease in the impact parameter and further decreases to the minimum value $-\pi$ as the impact parameter $J\rightarrow0$. Because of this behavior of the deflection angle gravitational lensing with SNS would give either two or nil Einstein rings and one RCC. As there are no photon spheres of SNS the deflection angles for these cases are never unboundedly large. Gravitational lensing by SNS would not give rise to relativistic images. In Fig. 3 (bottom left and right) we plot for some other values of ν for SNS.

In Table I we give the maximum deflection angle ($\hat{\alpha}_{max}$) that a light ray may suffer in the gravitational field of a strongly naked singularity and the corresponding impact parameter for many values of ν. As ν decreases (equivalently, q/M increases), $\hat{\alpha}_{max}$ decreases whereas the corresponding

V. GRAVITATIONAL LENSING BY MDOS AT GALACTIC CENTERS

We consider massive dark objects at different galactic centers, modeling them both as Schwarzschild black holes and as WNS and SNS, and study the gravitational lensing. We use the JNW metric to describe the WNS and SNS.

The deflection angle and the impact parameter of a light ray passing through the JNW gravitational field are respectively given by Eqs. (17) and (18). Introducing radial distance defined in terms of b,

$$\rho=\frac{r}{b}, \quad \rho_0=\frac{r_0}{b}, \tag{23}$$

the deflection angle $\hat{\alpha}$ and the impact parameter J assume the form

$$\hat{\alpha}(\rho_0)=2\int_{\rho_0}^{\infty}\frac{d\rho}{\rho\sqrt{1-\dfrac{1}{\rho}}\sqrt{\left(\dfrac{\rho}{\rho_0}\right)^2\left(1-\dfrac{1}{\rho}\right)^{1-2\nu}\left(1-\dfrac{1}{\rho_0}\right)^{2\nu-1}-1}}-\pi \tag{24}$$

and

$$J=2M\frac{\rho_0}{\nu}\left(1-\frac{1}{\rho_0}\right)^{(1-2\nu)/2}. \tag{25}$$

TABLE II. Mass and distance of MDOs at galactic centers.

Galaxies	Mass of MDO in $M_\odot$	Distance D_d in Mpc	$\dfrac{M}{D_d}$
Galaxy	2.8×10^6	0.0085	1.57×10^{-11}
NGC3115	2.0×10^9	8.4	1.14×10^{-11}
NGC4486 (M87)	3.3×10^9	15.3	1.03×10^{-11}
NGC4594 (M104)	1.0×10^9	9.2	5.20×10^{-12}
NGC4374 (M84)	1.4×10^9	15.3	4.37×10^{-12}
NGC0224 (M31)	3.0×10^7	0.7	2.05×10^{-12}
NGC4486B	5.7×10^8	15.3	1.78×10^{-12}
NGC4342 (IC3256)	3.0×10^8	15.3	9.37×10^{-13}
NGC3377	1.8×10^8	9.9	8.69×10^{-13}
NGC4261	4.5×10^8	27.4	7.85×10^{-13}
NGC3379 (M105)	6.7×10^7	9.9	3.24×10^{-13}
NGC7052	3.3×10^8	58.7	2.69×10^{-13}
NGC4258 (M106)	4.2×10^7	7.5	2.68×10^{-13}
NGC0221 (M32)	3.4×10^6	0.7	2.32×10^{-13}
NGC1068 (M77)	1.0×10^7	15.0	3.19×10^{-14}
NGC4945	1.4×10^6	3.7	1.81×10^{-14}

[Note that at $\rho_0=(2\nu+1)/2$ there is a photon sphere for $\nu:1/2<\nu\leqslant1$.]

Equation (25) with Eq. (3) give the image position θ by the expression

$$\sin\theta=\frac{2M}{D_d}\frac{\rho_0}{\nu}\left(1-\frac{1}{\rho_0}\right)^{(1-2\nu)/2}.\tag{26}$$

In computations to study gravitational lensing one requires the first derivative of the deflection angle $\hat{\alpha}$ with respect to θ. This is given by (see in [8])

$$\frac{d\hat{\alpha}}{d\theta}=\hat{\alpha}'(\rho_o)\frac{d\rho_o}{d\theta},\tag{27}$$

where

$$\frac{d\rho_o}{d\theta}=\frac{\nu\rho_0\left(1-\frac{1}{\rho_0}\right)^{(1+2\nu)/2}\sqrt{1-\frac{4}{\nu^2}\left(\frac{M}{D_d}\right)^2\rho_0^2\left(1-\frac{1}{\rho_0}\right)^{1-2\nu}}}{\frac{M}{D_d}(2\rho_0-2\nu-1)}\tag{28}$$

and the first derivative of $\hat{\alpha}$ with respect to ρ_0 is

$$\hat{\alpha}'(\rho_0)=\frac{2\nu+1-2\rho_0}{\rho_0^2\left(1-\frac{1}{\rho_0}\right)}\int_{\rho_0}^{\infty}\frac{(4\nu\rho-2\nu-1)d\rho}{(2\nu+1-2\rho)^2\rho\sqrt{1-\frac{1}{\rho}}\sqrt{\left(\frac{\rho}{\rho_0}\right)^2\left(1-\frac{1}{\rho}\right)^{1-2\nu}\left(1-\frac{1}{\rho_0}\right)^{2\nu-1}-1}}.\tag{29}$$

Table II gives a list of MDOs at some galactic centers, their masses and distances [17]. One can see that some of them have very close values for the ratio M/D_d, though they have different values of the mass M and distance D_d. As M/D_d plays a crucial role in the lensing (rather than M and D_d individually) lenses with close values of M/D_d, with the same value for D_{ds}/D_s, would give close results. Therefore, studying lensing due to one specific object may be helpful in estimating lensing effects due to others with a close value for M/D_d.

TABLE III. Critical curves and caustics due to lensing with the galactic MDO. (a) The lens is the galactic massive dark object (mass $M = 2.8 \times 10^6 M_\odot$ and the distance $D_d = 8.5$ kpc so that $M/D_d \approx 1.57 \times 10^{-11}$). (b) The ratio of the lens-source distance D_{ds} to the observer-source distance D_s is taken to be 1/2. θ_E, θ_r, and β_r stand for respectively the angular position of Einstein ring, radial critical curve, and radial caustic, whereas $\hat{\alpha}$ and J/M denote for the corresponding bending angle of the light ray and its impact parameter scaled in terms of the ADM mass. All angles are given in arcseconds.

	Inner Einstein ring			Outer Einstein ring			Radial critical curve and caustic			
ν	θ_E	$\hat{\alpha}$	J/M	θ_E	$\hat{\alpha}$	J/M	θ_r	$\hat{\alpha}$	J/M	β_r
1.0	$\times$	$\times$	$\times$	1.157544	2.315089	356386.33	$\times$	$\times$	$\times$	$\times$
0.8	$\times$	$\times$	$\times$	1.157544	2.315089	356386.28	$\times$	$\times$	$\times$	$\times$
0.6	$\times$	$\times$	$\times$	1.157544	2.315088	356386.16	$\times$	$\times$	$\times$	$\times$
0.05	0.000258	0.000515	79.329303	1.157417	2.314834	356347.16	0.000514	2641.816	158.12306	-1320.962
0.04	0.000401	0.000802	123.50606	1.157345	2.314691	356325.06	0.000801	1687.159	246.47827	-843.5928
0.03	0.000711	0.001422	218.95235	1.157190	2.314381	356277.30	0.001421	947.4574	437.37158	-473.7298
0.02	0.001597	0.003194	491.65985	1.156747	2.313494	356140.74	0.003192	420.5955	982.77908	-210.2948
0.01	0.006380	0.012760	1964.3395	1.154343	2.308686	355400.59	0.012757	105.0746	3927.5525	-52.52452
0.005	0.025525	0.051049	7858.5866	1.144573	2.289145	352392.53	0.050924	26.26390	15678.665	-13.08103
0.004	0.039909	0.079818	12287.235	1.137075	2.274151	350084.29	0.079349	16.80823	24429.955	-8.324767
0.002	0.162650	0.325300	50076.867	1.067618	2.135237	328699.81	0.298939	4.183341	92037.651	-1.792732
0.0002	$\times$	$\times$	$\times$	$\times$	$\times$	$\times$	3.368211	-2.970441	1037009.3	4.853431

Now we consider four MDOs at the centers of the Galaxy, NGC4486B, NGC0221 (M32) and NGC4945, and model them as the Schwarzschild black hole and the JNW naked singularities (WNS as well as SNS) and study the resulting gravitational lensing by them in detail. We use MATH-EMATICA [18] for computation. We consider a point source with the lens situated halfway between the source and the observer (i.e., $D_{ds}/D_s = 1/2$). Note that throughout this paper we assume D_{ds}/D_s to be fixed. We compute the angular positions of the tangential and radial critical curves, and radial caustics. We also compute the corresponding light deflection angles and the impact parameters (scaled in terms of the ADM mass M) of the light rays. The results are given in Tables III, IV, V and VI. For the Schwarzschild black holes ($\nu = 1$) as well as WNS ($\nu = 0.8, 0.6$) there is one Einstein ring and no RCC. The angular positions of the Einstein rings

for these cases, for a given value of M/D_d, decrease extremely slowly with an increase in the value of $(q/M)^2$ (i.e., with a decrease in the value of ν). It is worth noting that these have the same values up to the sixth decimal point when expressed in arcseconds. The size of an Einstein ring, for a given value of ν, decreases with a decrease in the value of M/D_d (cf. results in Tables III, IV, V and VI). The Schwarzschild black hole as well as WNS have a photon sphere. A light ray passing close to a photon sphere goes around once, twice, or many times depending on the impact parameter before reaching the observer. This gives rise to a large number of relativistic images. The sources of the entire universe are mapped in the vicinity of a photon sphere. In [9] we found that relativistic images are transient and are extremely demagnified and therefore are not of present observational interests. For the gravitational lensing due to WNS

TABLE IV. Critical curves and caustics due to lensing by the MDO in NGC4486B. (a) The lens is the massive dark object ($M = 5.7 \times 10^8 M_\odot$ and the distance $D_d = 15.3$ Mpc so that $M/D_d \approx 1.78 \times 10^{-12}$) in NGC4486B. (b) The same as (b) of Table III.

	Inner Einstein ring			Outer Einstein ring			Radial critical curve and caustic			
ν	θ_E	$\hat{\alpha}$	J/M	θ_E	$\hat{\alpha}$	J/M	θ_r	$\hat{\alpha}$	J/M	β_r
1.0	$\times$	$\times$	$\times$	0.389277	0.778554	1059736.0	$\times$	$\times$	$\times$	$\times$
0.8	$\times$	$\times$	$\times$	0.389277	0.778554	1059736.0	$\times$	$\times$	$\times$	$\times$
0.6	$\times$	$\times$	$\times$	0.389277	0.778554	1059735.8	$\times$	$\times$	$\times$	$\times$
0.05	0.000029	0.000058	79.329299	0.389263	0.778525	1059696.8	0.000058	2641.816	158.12308	-1320.962
0.04	0.000045	0.000091	123.50605	0.389254	0.778509	1059674.7	0.000091	1687.159	246.47838	-843.5935
0.03	0.000080	0.000161	218.95228	0.389237	0.778474	1059627.0	0.000161	947.4574	437.37216	-473.7310
0.02	0.000181	0.000361	491.65902	0.389187	0.778374	1059490.6	0.000361	420.5955	982.78568	-210.2976
0.01	0.000722	0.001443	1964.2866	0.388916	0.777832	1058753.0	0.001443	105.0746	3927.9751	-52.53584
0.005	0.002885	0.005771	7855.1974	0.387826	0.775653	1055787.1	0.005769	26.26400	15705.553	-13.12623
0.004	0.004509	0.009018	12274.277	0.387003	0.774006	1053546.0	0.009011	16.80860	24531.587	-8.395287
0.002	0.018071	0.036141	49194.177	0.379927	0.759854	1034282.7	0.035762	4.201732	97354.227	-2.065105
0.0002	$\times$	$\times$	$\times$	$\times$	$\times$	$\times$	0.755914	-0.555448	2057839.3	1.033638

TABLE V. Critical curves and caustics due to lensing by the MDO in NGC0221. (a) The lens is the massive dark object ($M = 3.4 \times 10^6 M_\odot$ and the distance $D_d = 0.7$ Mpc so that $M/D_d \approx 2.32 \times 10^{-13}$) in NGC0221. (b) The same as (b) of Table III.

| | Inner Einstein ring | | | Outer Einstein ring | | | Radial critical curve and caustic | | | |
ν	θ_E	$\hat{\alpha}$	J/M	θ_E	$\hat{\alpha}$	J/M	θ_r	$\hat{\alpha}$	J/M	β_r
1.0	$\times$	$\times$	$\times$	0.140558	0.281117	2934935.6	$\times$	$\times$	$\times$	$\times$
0.8	$\times$	$\times$	$\times$	0.140558	0.281117	2934935.6	$\times$	$\times$	$\times$	$\times$
0.6	$\times$	$\times$	$\times$	0.140558	0.281117	2934935.5	$\times$	$\times$	$\times$	$\times$
0.05	0.000004	0.000008	79.329299	0.140557	0.281113	2934896.5	0.000008	2641.816	158.12309	-1320.962
0.04	0.000006	0.000012	123.50605	0.140556	0.281111	2934874.4	0.000012	1687.159	246.47839	-843.5936
0.03	0.000010	0.000021	218.95227	0.140553	0.281106	2934826.6	0.000021	947.4574	437.37222	-473.7312
0.02	0.000024	0.000047	491.65893	0.140547	0.281093	2934690.3	0.000047	420.5955	982.78641	-210.2979
0.01	0.000094	0.000188	1964.2807	0.140511	0.281023	2933953.5	0.000188	105.0746	3928.0220	-52.53709
0.005	0.000376	0.000752	7854.8222	0.140370	0.280740	2931000.8	0.000752	26.26400	15708.551	-13.13125
0.004	0.000588	0.001176	12272.845	0.140264	0.280527	2928780.4	0.001175	16.80860	24543.015	-8.403126
0.002	0.002352	0.004703	49101.913	0.139368	0.278736	2910077.1	0.004697	4.202026	98066.326	-2.096317
0.0002	$\times$	$\times$	$\times$	$\times$	$\times$	$\times$	0.179149	-0.068868	3740727.3	0.213583

we computed magnifications of relativistic images. We found that, as expected, these images are highly demagnified. For this reason we do not present them in the tables.

For the SNS cases ($0 \leq \nu \leq 1/2$ or equivalently $q^2 \geq 3M^2$) there are double or nil Einstein rings, but there is always one RCC. For a given M/D_d, the size of the inner Einstein ring (when it is present) increases whereas that of the outer Einstein ring decreases with an increase in the value of $(q/M)^2$ (i.e., with a decrease in the value of ν). As the value of $(q/M)^2$ increases the separation between the two Einstein rings decreases and these coalesce for a certain value of $(q/M)^2$, which depends on the value of M/D_d. For any larger value of $(q/M)^2$ there will be no Einstein rings, but there will always be one RCC. For a fixed value of M/D_d, the angular position of a RCC increases with an increase in the value of $(q/M)^2$. (The negative angular position for the radial caustics implies that the source is on the

opposite side of the RCC.) The angular positions of the radial caustics have negative values unless $(q/M)^2$ is large; the value of $(q/M)^2$ for which the RC becomes positive depends on the value of M/D_d. Though we do not present in the tables the results for the purely scalar field ($\nu=0$, i.e., $M=0$ but $q \neq 0$), we find that for any value of M/D_d and scalar charge there are no Einstein rings, but there is always one RC; angular positions of the RCC as well as RC have the same sign and thus the source and images are on the same side of the optic axis. In Figs. 4, 5 and 6 we plot the tangential, radial, and the total magnifications of images with respect to the image position when the lenses are the galactic MDO modeled as a Schwarzschild black hole, WNS ($\nu=0.6$) and SNS ($\nu=0.002, 0.001$).

Figure 4 shows that the lensing due to a Schwarzschild black hole and WNS are not only qualitatively the same in that they have only one Einstein ring and no RCC, but the magnifications of an image at a given angular position also
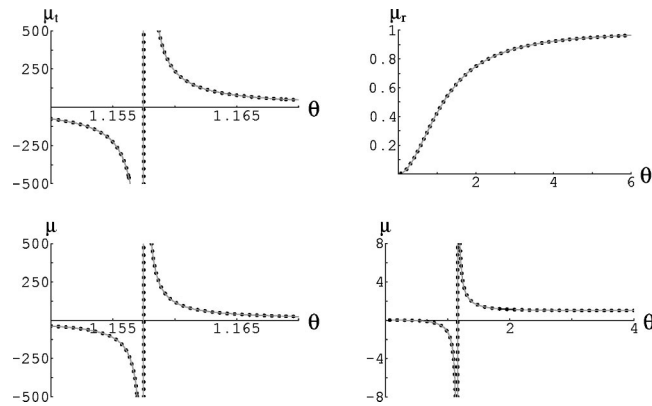

FIG. 4. The *tangential magnification* μ_t, *radial magnification* μ_r, and *total magnification* μ are plotted against the image position θ. The galactic MDO ($M/D_d \approx 1.57 \times 10^{-11}$) is modeled as a Schwarzschild black hole as well as a WNS ($\nu=0.6$) lens. The dotted and continuous curves are respectively for the gravitational lensing due to the Schwarzschild black hole and the WNS. $D_{ds}/D_s = 1/2$ and the image positions are expressed in arcseconds.
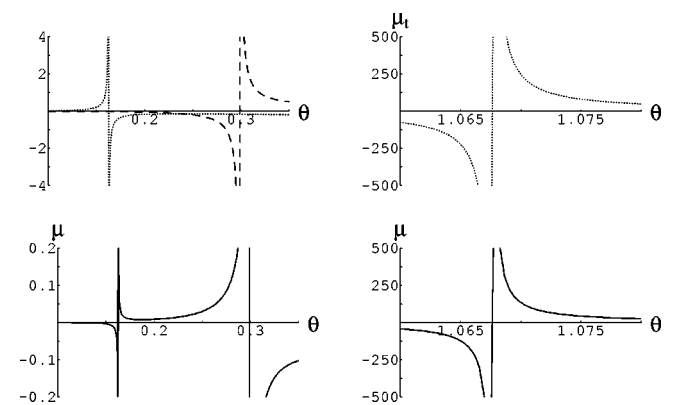

FIG. 5. The *tangential magnification* μ_t (represented by dotted curves), *radial magnification* μ_r (represented by dashed curves), and *total magnification* μ (represented by continuous curves) are plotted against the image position θ (in arcseconds). The galactic MDO ($M/D_d \approx 1.57 \times 10^{-11}$) is modeled as a WNS ($\nu=0.002$) lens and $D_{ds}/D_s = 1/2$.
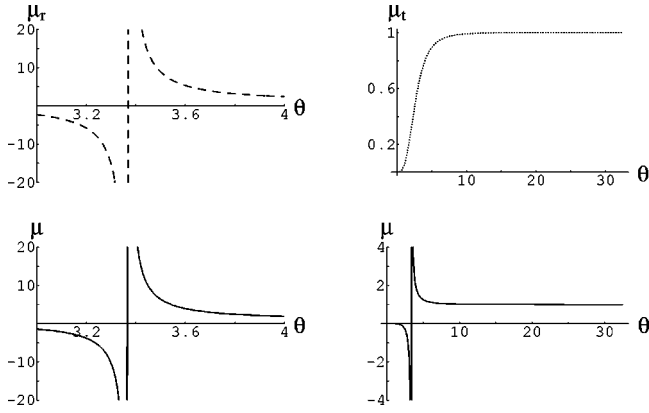
FIG. 6. The *radial magnification* μ_r (represented by dashed curves), *radial magnification* μ_t (represented by dotted curves), and *total magnification* μ (represented by continuous curves) are plotted as a function of the image position θ (in arcseconds). The galactic MDO ($M/D_d \approx 1.57 \times 10^{-11}$) is modeled as a WNS ($\nu = 0.0002$) lens and $D_{ds}/D_s = 1/2$.

have very close values. The image on the same or opposite side of the source has positive or negative tangential parity whereas the radial parity of all the images are positive.

Figure 5 shows that for a SNS ($\nu = 0.002$) lensing there are two Einstein rings and one RCC. The rate of fall of magnification with respect to a change in the image position near the inner TCC is more than that near the outer TCC; consequently, the inner Einstein ring will appear fainter compared to the outer ring. Figure 6 shows the variation of magnifications as a function of the image position due to a WNS ($\nu = 0.0002$) lensing. In this case there is no Einstein ring, but one RCC.

VI. SUMMARY

Despite serious efforts over the past three decades no general proof for the CCH is obtained, and on the other hand no convincing counterexample to this hypothesis is known. However, recent studies of *type Ia* supernovae indicating a

positive cosmological constant have by implication called the CCH into question. Therefore, it is now a pressing need of astrophysics that distinctive observational features of black holes and naked singularities be investigated theoretically. Gravitational lenses, also known as cosmic telescopes, may play an important role in unveiling and understanding these exotic and esoteric objects if these indeed exist in the universe. We addressed this problem and encouraging results have emerged. We considered Schwarzschild black holes and JNW naked singularities. The null geodesic structure and consequently gravitational lensing in the gravitational field of a Schwarzschild black hole as well as a WNS have been found to share the same qualitative features; however, these features differ substantially for a SNS. Gravitational lensing features due to a Schwarzschild black hole, WNS, and SNS are summarized below.

Schwarzschild black hole and WNS. Gravitational lensing by these objects give rise to one Einstein ring when the lens components (source, lens and observer) are aligned. As the alignment is ''broken'' the ring splits into two images (one on each side of the optic axis). Gravitational lensing by these lenses have no radial caustic.

Because of the existence of a photon sphere with a Schwarzschild black hole or a WNS, gravitational lensing by these gives rise to a sequence of a large number of closely packed highly demagnified relativistic Einstein rings when the lens components are aligned. As the lens components deviate from their alignment, each relativistic ring splits into two relativistic images. The magnifications of these images decrease very fast as the angular position of the source increases.

SNS. When the lens components are aligned, gravitational lensing by a SNS gives rise to two or nil Einstein ring(s). In the case of double rings the inner ring is fainter compared to the outer one. Gravitational lensing by a SNS has a radial caustic, but no relativistic images.

When the lens components are not aligned, a SNS lensing may give rise to two or four lensed images. Both lensed images are on the same side as the light source for the

TABLE VI. Critical curves and caustics due to lensing by the MDO in NGC4945. (a) The lens is the massive dark object ($M = 1.4 \times 10^6 M_\odot$ and the distance $D_d = 3.7$ Mpc so that $M/D_d \approx 1.81 \times 10^{-14}$) in NGC4945. (b) The same as (b) of Table III.

	Inner Einstein ring			Outer Einstein ring			Radial critical curve and caustic			
ν	θ_E	$\hat{\alpha}$	J/M	θ_E	$\hat{\alpha}$	J/M	θ_r	$\hat{\alpha}$	J/M	β_r
1.0	$\times$	$\times$	$\times$	0.039231	0.078462	10515397.8	$\times$	$\times$	$\times$	$\times$
0.8	$\times$	$\times$	$\times$	0.039231	0.078462	10515397.7	$\times$	$\times$	$\times$	$\times$
0.6	$\times$	$\times$	$\times$	0.039231	0.078462	10515397.6	$\times$	$\times$	$\times$	$\times$
0.05	0.0000003	0.0000006	79.329299	0.039231	0.078462	10515358.6	0.0000006	2641.816	158.12309	-1320.962
0.04	0.0000005	0.0000009	123.50605	0.039231	0.078462	10515336.5	0.0000009	1687.159	246.47839	-843.5936
0.03	0.0000008	0.000002	218.95227	0.039231	0.078461	10515288.8	0.000002	947.4574	437.37223	-473.7312
0.02	0.000002	0.000004	491.65892	0.039230	0.078460	10515152.4	0.000004	420.5955	982.78652	-210.2980
0.01	0.000007	0.000015	1964.2799	0.039227	0.078455	10514416.0	0.000015	105.0746	3928.0284	-52.53727
0.005	0.000029	0.000059	7854.7703	0.039216	0.078433	10511468.7	0.000059	26.26400	15708.966	-13.13194
0.004	0.000046	0.000092	12272.647	0.039208	0.078416	10509256.6	0.000092	16.80860	24544.597	-8.404209
0.002	0.000183	0.000366	49089.239	0.039139	0.078278	10490767.7	0.000366	4.202032	98167.253	-2.100650
0.0002	$\times$	$\times$	$\times$	$\times$	$\times$	$\times$	0.025655	0.034335	6876621.4	0.008488

double-image case, while for the quadruple case, two lensed images are on each side of the optic axis.

It is significant that the Einstein bending angle $\hat{\alpha}$ of a light ray necessarily approaches the value $-\pi$ as the closest distance of approach r_0 tends to the singularity.

As gravitational lensing by a Schwarzschild black hole as well as a WNS share the same qualitative features and their quantitative values are also very close (see Fig. 4 and Tables III–VI), it may not be possible to differentiate observationally a WNS from a Schwarzschild black hole. However, as gravitational lensing by a SNS has quite different qualitative features, it can be easily differentiated from a Schwarzschild black hole lensing.

Our studies of gravitational lensing by black holes and naked singularities are limited to spherically symmetric spacetimes. Rauch and Blandford [19] did some studies of Kerr black hole weak field gravitational lensing. It is of interest to investigate photon surfaces of the Kerr metric and their role (if they exist) in gravitational lensing by Kerr black holes and Kerr naked singularities.

ACKNOWLEDGMENTS

[1] R. Penrose, Riv. Nuovo Cimento **1**, 252 (1969).

[2] R. Penrose, in *General Relativity and Einstein Centenary Survey*, edited by S. W. Hawking and W. Israel (Cambridge University Press, Cambridge, England, 1979).

[3] R.M. Wald, ''Gravitational Collapse and Cosmic Censorship,'' gr-qc/9710068.

[4] R. Penrose, in *Black Holes and Relativistic Stars*, edited by R. M. Wald (University of Chicago Press, Chicago, 1998), p. 103.

[5] K.S. Virbhadra, Phys. Rev. D **60**, 104041 (1999).

[6] A.G. Riess *et al.*, Astron. J. **116**, 1009 (1998); S. Perlmutter *et al.*, Astrophys. J. **517**, 565 (1999); I. Zehavi and A. Dekel, Nature (London) **401**, 252 (1999); A. Filippenko and A. Riess, ''Type Ia Supernovae and Their Cosmological Implications,'' astro-ph/9905049.

[7] L. Wang, R.R. Caldwell, J.P. Ostriker, and P.J. Steinhardt, Astrophys. J. **530**, 17 (2000), and references therein.

[8] K.S. Virbhadra, D. Narasimha, and S.M. Chitre, Astron. Astrophys. **337**, 1 (1998); S. Weinberg, *Gravitation and Cosmology: Principles and Applications of the General Theory of Relativity* (Wiley, New York, 1972).

[9] K.S. Virbhadra and G.F.R. Ellis, Phys. Rev. D **62**, 084003 (2000).

[10] S. Frittelli, T.P. Kling, and E.T. Newman, Phys. Rev. D **61**, 064021 (2000).

[11] P. Schneider, J. Ehlers, and E. E. Falco, *Gravitational Lenses* (Springer-Verlag, Berlin, 1992); A. O. Petters, H. Levine, and J. Wambsganss, *Singularity Theory and Gravitational Lensing* (Birkhauser, Boston, 2001).

[12] C.-M. Claudel, K.S. Virbhadra, and G.F.R. Ellis, J. Math. Phys. **42**, 818 (2001).

[13] K.S. Virbhadra, Int. J. Mod. Phys. A **12**, 4831 (1997).

[14] A.I. Janis, E.T. Newman, and J. Winicour, Phys. Rev. Lett. **20**, 878 (1968).

[15] M. Wyman, Phys. Rev. D **24**, 839 (1981).

[16] K.S. Virbhadra, S. Jhingan, and P.S. Joshi, Int. J. Mod. Phys. D **6**, 357 (1997).

[17] D. Richstone *et al.*, Nature (London) **395**, A14 (1998).

[18] S. Wolfram, MATHEMATICA 4.0.

[19] K.P. Rauch and R.D. Blandford, Astrophys. J. **421**, 46 (1994).

[20] Until recently this solution was known as the Wyman solution. In [13] it is shown that this solution was obtained in different coordinates by Janis, Newman, and Winicour [14] about thirteen years before Wyman [15].

[21] In [9] *relativistic Einstein rings* are defined as those which are formed due to light deflection by more than 2π. Similarly, images which are formed due to light deflection by more than $3\pi/2$ are termed *relativistic images*.